LS-DYNA® material model 263 and its application to earing predictions in cup-drawing

Jinglin Zheng[1*], Yanshan Lou[2], Xinhai Zhu[1], Saijun Zhang[3], Jeong Whan Yoon[4]

1 Livermore Software Technology Corporation, 7374 Las Positas Road, Livermore, CA 94551, U.S.A.

2 School of Mechanical Engineering, Xi'an Jiao Tong University, 28 Xianning West Road, Xi'an, Shaanxi 710049, China

3 Guangdong provincial Key Laboratory of Precision Equipment and Manufacturing Technology, School of Mechanical and Automotive Engineering, South China University of Technology, Guangzhou 510640, China

4 Department of Mechanical Engineering, Korea Advanced Institute of Science and Technology (KAIST), 291 Daehak-ro, Yuseong-gu, Daejeon, 305-701, Republic of Korea

Abstract This paper introduces a newly implemented metal forming material model, material type 263, in LS-DYNA® material library. The yield function of this model is based on a recent theoretical development of extending the original Drucker function into an anisotropic form. The flexibility of the yield function is further improved by adopting the non-associated flow rule. The paper also outlines how to use LS-OPT® to calibrate the material parameters used in the model, followed by a cup-drawing analysis which demonstrates the model's capability of capturing the cup earing profile, especially when paired with LS-OPT® for material parameter identification.

摘要: 本文介绍了 LS-DYNA®材料库中最新植入的金属成形材料模型，材料标号为 263。该材料模型的屈服函数是基于最近提出的、把最初的 Drucker 方程扩展到各向异性的理论方法。该屈服方程的柔性能够通过采用非关联流动准则来进一步提高。本文还概述了如何使用 LS-OPT®来标定模型中的材料参数，并将标定后的材料参数用于进行杯凸实验的有限元分析。杯凸有限元分析结果与实验结果的对照表明该模型具有准确预测杯凸轮廓的能力，特别是在屈服函数的参数通过 LS-OPT®标定的情况下，参数标定和有限元分析所采用的数值算法的一致性进一步提高了杯凸轮廓预测的准确性。

1. Introduction

Over the years LS-DYNA® has been making efforts to keep an up-to-date material library to satisfy the ever-growing customers' needs for precise characterization of material behaviors under various loading conditions. This paper focuses on a newly implemented metal forming material model, material type 263 (*MAT_LOU-YOON_ANISOTROPIC_PLASTICITY), based on the anisotropic yield function recently proposed by Lou and Yoon [1]. This yield function extends the original Drucker function into an anisotropic form using a fourth order linear transformation tensor. As a stress-invariant-based yield criterion, the anisotropic Drucker yield function is less computationally expensive compared to the principle-stress-based yield functions, especially in the spatial loading cases. In the meantime, the non-associated flow rule (non-AFR) is applied to accurately characterize both the directional yield stresses and R-values while keeping the model simple and efficient. The anisotropic flexibility of this model can be further improved by summing up more components of the anisotropic Drucker function. Last but not least, the *c*-value in the Drucker function is calibrated for body-centered cubic (BCC) and face-centered cubic (FCC) metals for the first time thereby endowing the function with the identical capability to non-quadratic yield functions to differentiate distinct plastic behaviors between BCC and FCC metals.

This paper gives a brief review on the anisotropic Drucker yield function and its implementation in LS-DYNA®, then a demonstration on how to calibrate the input material parameters using LS-OPT®, followed by a numerical simulation based on the new material model to predict earing during a cup-drawing process. The simulation demonstrates excellent agreement with measured data, especially when paired with LS-OPT® for material parameter calibration.

2. Anisotropic yield criterion based on Drucker function

Drucker proposed a yield function by including the third stress invariant into the classical Von Mises yield function [2]. The Drucker function is extended to an anisotropic form as shown below[1]:

$$\bar{\sigma}_y(\sigma_{ij}) = (J'^3_2 - cJ'^2_3)^{1/6} \tag{1}$$

where J'_2 and J'_3 are the second and third invariants of the linear transformed deviatoric stress tensor $\boldsymbol{s}'$:

$$\boldsymbol{s}' = \boldsymbol{L}'\boldsymbol{\sigma} \tag{2}$$

The fourth order linear transformation tensor $\boldsymbol{L}'$ in equation (2) is given by:

$$\boldsymbol{L}' = \begin{bmatrix} (c'_2+c'_3)/3 & -c'_3/3 & -c'_2/3 & 0 & 0 & 0 \\ -c'_3/3 & (c'_1+c'_3)/3 & -c'_1/3 & 0 & 0 & 0 \\ -c'_2/3 & -c'_1/3 & (c'_2+c'_1)/3 & 0 & 0 & 0 \\ 0 & 0 & 0 & c'_4 & 0 & 0 \\ 0 & 0 & 0 & 0 & c'_5 & 0 \\ 0 & 0 & 0 & 0 & 0 & c'_6 \end{bmatrix} \tag{3}$$

The coefficient c in equation (1) is calibrated to be 1.226 for metals with BCC and 2 for FCC [1]. c'_1, c'_2, c'_3 and c'_6 in equation (3) can be calibrated from uniaxial tensile yield stress along different directions and the balanced biaxial yield stress. On the other hand, c'_4 and c'_5 , which are related to the through-thickness material properties, are very difficult to obtain experimentally and therefore assumed to be identical with c'_6.

The fact that only six anisotropic parameters are to be identified makes the flexibility of equation (1) comparable to Hill48 and Yld91 functions [1]. A way to improve this is to adopt the non-associated flow rule (non-AFR), in which the plastic flow is not required to be aligned with the yield surface normal and the *r*-values are modeled by a different plastic potential as shown in equation (4):

$$\bar{\sigma}_p(\sigma_{ij}) = (\hat{J}^3_2 - c\hat{J}^2_3)^{1/6} \tag{4}$$

where $\hat{J}_2$ and $\hat{J}_3$ are the second and third invariants of the linear transformed deviatoric stress tensor $\hat{\boldsymbol{s}}$:

$$\hat{\boldsymbol{s}} = \hat{\boldsymbol{L}}\boldsymbol{\sigma} \tag{5}$$

with $\hat{\boldsymbol{L}}$ defined as:

$$\hat{\boldsymbol{L}} = \begin{bmatrix} (\hat{c}_2+\hat{c}_3)/3 & -\hat{c}_3/3 & -\hat{c}_2/3 & 0 & 0 & 0 \\ -\hat{c}_3/3 & (\hat{c}_1+\hat{c}_3)/3 & -\hat{c}_1/3 & 0 & 0 & 0 \\ -\hat{c}_2/3 & -\hat{c}_1/3 & (\hat{c}_2+\hat{c}_1)/3 & 0 & 0 & 0 \\ 0 & 0 & 0 & \hat{c}_4 & 0 & 0 \\ 0 & 0 & 0 & 0 & \hat{c}_5 & 0 \\ 0 & 0 & 0 & 0 & 0 & \hat{c}_6 \end{bmatrix} \tag{6}$$

The anisotropic parameters $\hat{c}_1$, $\hat{c}_2$, $\hat{c}_3$ and $\hat{c}_6$in equation (6) can be calibrated with experimentally measured *r*-values along different directions.

Another approach to improve the flexibility of equation (1) is to sum up n components of the anisotropic Drucker functions as follows [1]:

$$\bar{\sigma}_y(\sigma_{ij}) = \frac{1}{n}\sum_{m=1}^{n}\{[(J_2'^{(m)})^3 - c(J_3'^{(m)})^2]^{1/6}\} \quad (7)$$

with the integer $n \geq 1$. The same idea can be applied to the plastic potential in the non-AFR approach, as shown by equation (8):

$$\bar{\sigma}_p(\sigma_{ij}) = \frac{1}{n}\sum_{m=1}^{n}\{[(\hat{J}_2^{(m)})^3 - c(\hat{J}_3^{(m)})^2]^{1/6}\} \quad (8)$$

The accuracy of equations (7) and (8) improves as n increases.

3. LS-DYNA® model implementation and material parameter identification

The material model is implemented as material type 263 in LS-DYNA® material library and can be accessed with the keyword *MAT_263 or *MAT_LOU-YOON_ANISOTROPIC_PLASTICITY. Both AFR and non-AFR options are available. Currently, the allowed number of Drucker functions is limited to one. Various hardening laws are implemented including Swift, Voce, Gosh, and Hocken-Sherby. Alternatively, a customized hardening curve can also be imported to characterize the material's hardening behavior as a function of the effective plastic strain. Details on the card structure of this keyword can be found in the keyword manual of LS-DYNA®.

One essential step to apply this material model to a real analysis is determination of the anisotropic parameters. In the case of one Drucker function, this keyword requires input of a total of 4 anisotropic parameters (c_1', c_2', c_3', c_6') in the AFR case. With the non-AFR option, four more anisotropic parameters ($\hat{c}_1$, $\hat{c}_2$, $\hat{c}_3$, $\hat{c}_6$) are to be defined. As briefly mentioned in section 2, these anisotropic parameters should be calibrated from yield stresses and *r*-values measured from uniaxial tensile tests loaded at different angles and the balanced bi-axial tensile test. However, the procedures of identifying these parameters from measured data are not standardized across the industry. As the key idea is to find the best parameter set that reproduces the material's yield behavior as close as possible, here we use LS-OPT®, a LS-DYNA®-based general optimization program developed by Livermore Software Technology Corporation, to determine the anisotropic parameter set required by material type 263.

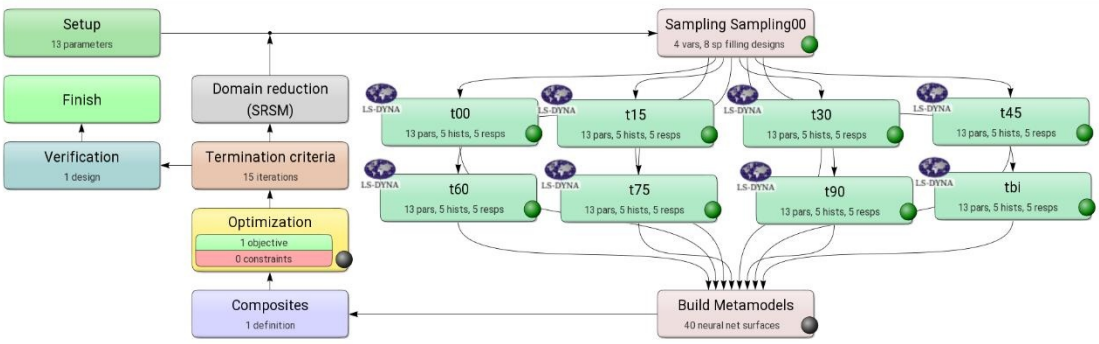

Figure 1 A schematic view of LS-OPT® setup to calibrate anisotropic parameters of material type 263

Figure 1 illustrates the structure of a material parameter identification project built in LS-OPT®. The key steps of setting up this project include: (1) set up the parameters to be identified, and in this case, the anisotropic parameter set (c_1', c_2', c_3', c_6'); (2) set up a series of simulation stages which predicts

the material's yield behavior under experimental conditions, and in this case, a total of eight stages, including 7 uniaxial tensile tests, in the direction of 0°, 15°, 30°, 45°, 60°, 75° and 90° respectively, and one balanced bi-axial tensile test, are set up in the project; (3) set up the optimization objective, which is to minimize an error function (termed as composite in LS-OPT®) which measures the differences in yield stresses predicted by the model and observed from experiments. The definition of the error function is given by equation (9):

$$\mathrm{F} = \sum_{\theta=0}^{90}\left(\frac{\sigma_\theta}{\sigma_\theta^{pred}} - 1\right)^2 + \left(\frac{\sigma_b}{\sigma_b^{pred}} - 1\right)^2 \tag{9}$$

where σ_θ and σ_b are yield stresses obtained from uniaxial and biaxial tensile tests, and σ_θ^{pred} and σ_b^{pred} are LS-DYNA® predicted values using material model 263. Note that the finite element model used in these simulation stages contains only one single element to accelerate the optimization process. This particular optimization project is set up to identify the anisotropic parameters of an aluminum alloy 2008-T4, which is known as an FCC material with moderate anisotropy. Accordingly, *c* is set to 2 in the anisotropic Drucker function. The experimental yield stresses for this material can be found from the literature and are listed in Table 1.

Table 1 Experimental yield stresses and *r*-values of AA2008-T4 [3]

σ_0/σ_0	σ_{15}/σ_0	σ_{30}/σ_0	σ_{45}/σ_0	σ_{60}/σ_0	σ_{75}/σ_0	σ_{90}/σ_0	σ_b/σ_0
1.0000	0.9963	0.9835	0.9459	0.9303	0.9171	0.9044	0.9010
r_0	r_{15}	r_{30}	r_{45}	r_{60}	r_{75}	r_{90}	r_b
0.8674	0.8077	0.6188	0.4915	0.4955	0.5114	0.5313	1.0000

The parameter set (c_1', c_2', c_3', c_6') optimized by LS-OPT® is listed in Table 2 and the predicted yield stresses based on this parameter set are compared with experimental values in Figure 2(a).

Table 2 LS-OPT® optimized anisotropic parameter values and parameter values found from the literature [3]

	c_1'	c_2'	c_3'	c_6'	$\hat{c}_1$	$\hat{c}_2$	$\hat{c}_3$	$\hat{c}_6$
By LS-OPT® (case I)	2.2511	1.8141	1.7885	1.8005	2.0505	1.7656	1.7095	1.6955
From literature [3] (cases II and III)	2.2190	1.8448	1.8282	1.9082	2.1913	1.8729	1.7995	1.7829

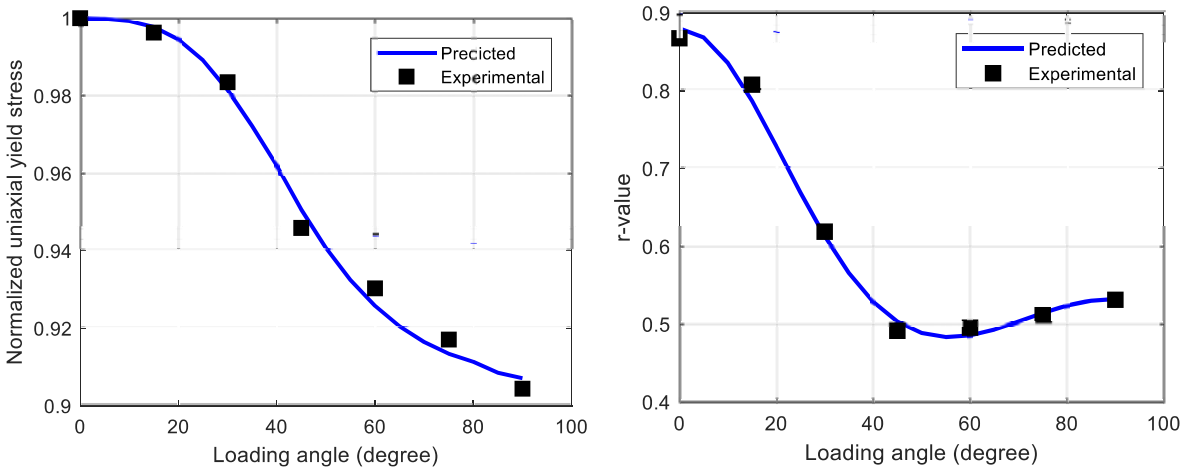

(a) yield stresses at different (b) r-values at different loading

Figure 2 Yield stresses and *r*-values predicted by LS-DYNA® as compared to experimental data

In a similar manner, we can setup another optimization project to identify the values of ($\hat{c}_1$, $\hat{c}_2$, $\hat{c}_3$, $\hat{c}_6$) by turning on the non-AFR option of material type 263. In this case, the optimization goal is to minimize an error function that evaluates the differences between predicted and measured *r*-values at different loading conditions, as shown in equation (10):

$$\mathrm{F} = \sum_{\theta=0}^{90}\left(\frac{r_\theta}{r_\theta^{pred}} - 1\right)^2 + \left(\frac{r_b}{r_b^{pred}} - 1\right)^2 \tag{10}$$

The values of ($\hat{c}_1$, $\hat{c}_2$, $\hat{c}_3$, $\hat{c}_6$) after LS-OPT® optimization are listed in Table 2 and Figure 2(b) plots the predicted *r*-values based on the optimized parameter set as compared to the experimental values. As a reference, we also listed the anisotropic parameters for AA2008-T4 found from the literature [3] in Table 2. As expected, the values are close but not identical, due to the fact that (1) results by LS-OPT® are based on LS-DYNA®'s implementation of the theoretical model, i.e., material type 263; (2) different numerical procedures are employed during the optimization process; (3) optimization usually finds a local minimum which is dependent on the search range and initial guess.

4. Application to predict earing during a cup-drawing process

Based on the anisotropic parameter set identified by LS-OPT® in Section 3, a cup-drawing simulation using material type 263 is conducted to predict the final earing profile. The model contains only one quarter section of the cup. Dimensions of the tools and blank are given in detail in Yoon et al. (2006) [4]. The initial blank has a radius of 81 mm and is meshed with 3-dimensional solid elements. Element formulation 2 (with selective reduced integration, see LS-DYNA® user's manual for details) is applied in the analysis. Assuming isotropic hardening, the Voce hardening law is used to characterize the material's hardening behavior after yielding, as shown by equation (11):

$$\sigma_y = 408 - 175e^{-6.14\epsilon_p} \tag{11}$$

where ϵ_p stands for the effective plastic strain. Figure 3 shows the deformed cup shape after fully drawn with the contour of ϵ_p being plotted.

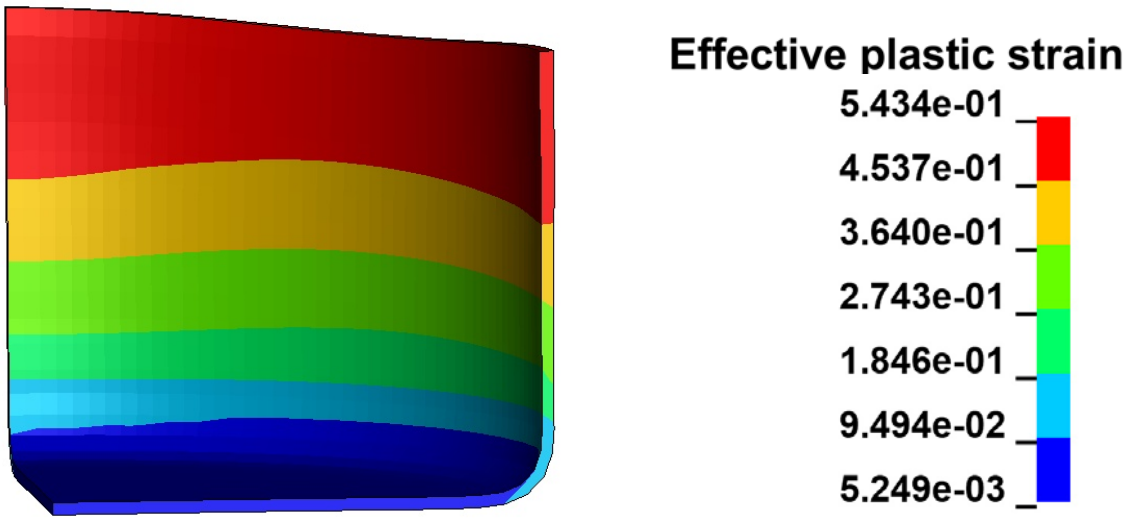

Figure 3 Simulated cup deformation after fully drawn with the contour of effective plastic strain

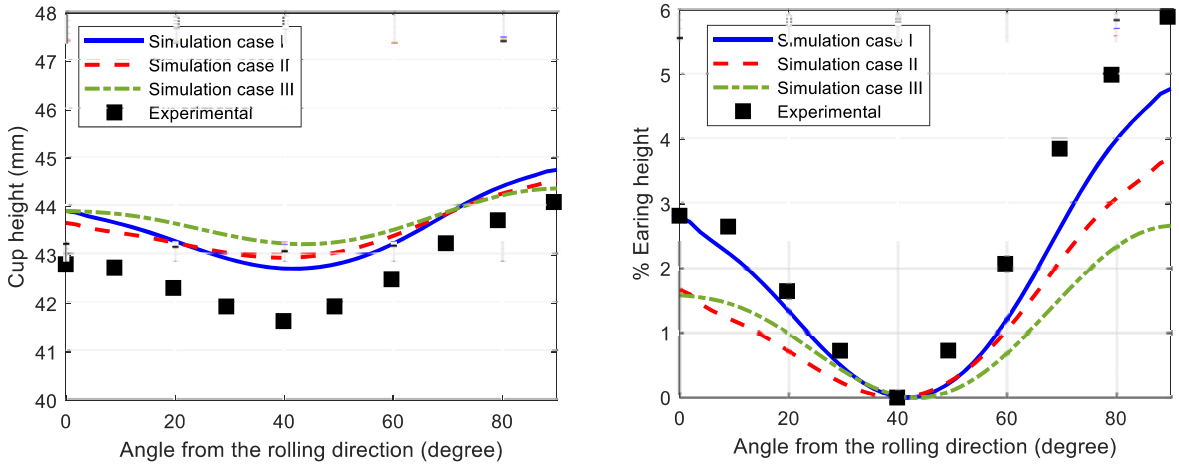

(a) Cup height after fully drawn

(b) Normalized earing profile

Figure 4 Simulation-predicted earing profile as compared to experimental results

To show how the model prediction correlates to experiments, Figure 4(a) compares three cases of simulated cup height as a function of the angle from the rolling direction along with the experimental data. Case I is obtained by using LS-DYNA® with the anisotropic parameters identified by LS-OPT® as listed in Table 2 (1st row). Case II is also calculated by LS-DYNA® but with the anisotropic parameters taken from the literature, which are also listed in Table 2 (2nd row). As a reference, another simulated profile, which is based on the same model with the same set anisotropic parameters as case II but uses a different numerical implementation [3], is included as case III. To better observe the variation of cup height, Figure 4(b) compares the % earing height of all three cases with the experimental data, where % earing height is calculated by equation (12):

$$\%\ \text{earing height} = \frac{Cup\ \ height - minimum\ \ cup\ \ height}{minimum\ \ cup\ \ height} \times 100 \qquad (12)$$

As illustrated by Figures 4(a) and (b), all three simulated cases are able to capture the general features of the overall earing profile. The differences between case II and case III are considered to be due to differences in the details of numerical implementation of the same theoretical model, as well as

different element formulations, contact assumptions, etc.. On the other hand, the differences between case I and II are solely caused by different sets of anisotropic parameters being used in the simulations. Case I, which uses the LS-OPT® identified parameters matches the experimental data better in terms of both the cup height values and the overall earing profile. The reason is considered to be the fact that the numerical algorithm used in the material parameter identification process and the cup-drawing analysis are consistent with each other. In case I, the LS-OPT® identification procedure serves as a "training" process that makes the material model 263 "learns" the best set of anisotropic parameters that matches the real material behavior. The numerical consistency between the identification process and simulation process leads to the overall improvement of earing prediction.

5. Conclusion

A new metal forming material model is implemented in LS-DYNA® material library as material type 263, accessed by the keyword *MAT_LOU-YOON_ANISOTROPIC_PLASTICITY, based on the theoretical model proposed by Lou and Yoon in 2018. The yield criterion of this model uses the stress-invariant-based Drucker function and the flexibility can be easily extended with the non-AFR option and/or further addition of Drucker components. The general procedures of using LS-OPT® to identify the anisotropic parameter set used as the model input are outlined. The model is then subject to a deep cup-drawing analysis on an aluminum alloy 2008-T4 blank and the prediction on the final earing profile is in good agreement with experimental results, especially when the analysis is paired with LS-OPT® identified anisotropic parameters.

Acknowledgement

The authors would like to thank Anirban Basudhar and Imtiaz Gandikota at Livermore Software Technology Corporation for their helpful advice on using LS-OPT® for material parameter identification.

References

[1] Lou Y, Yoon JW. Anisotropic yield function based on stress invariants for BCC and FCC metals and its extension to ductile fracture criterion. Int. J. Plast. 2018; 101:125-155.

[2] Drucker DC. Relations of experiments to mathematical theories of plasticity. J. Appl. Mech. 1949; 16: 349-357

[3] Lou Y, Zhang S, Yoon JW. A reduced Yld2004 function for modeling anisotropic plastic deformation of metals under triaxial loading. Int. J. Mech. Sci. Accepted.

[4] Yoon JW, Barlat F, Dick RE, Chuang K, Kang TJ. Prediction of six or eight ears in a drawn cup based on a new anisotropic yield function. Int. J. Plast. 2006; 22: 174-193